Smart Structures and Systems, *Vol. 17, No. 2 (2016) 209-230*
DOI: http://dx.doi.org/10.12989/sss.2016.17.2.209

Operational modal analysis of Canton Tower by a fast frequency domain Bayesian method

Feng-Liang Zhang[1a], Yi-Qing Ni[2b], Yan-Chun Ni [*1] and You-Wu Wang[2c]

[1]*Research Institute of Structural Engineering and Disaster Reduction, Tongji University, 1239 Siping Road, Shanghai, China*
[2]*Department of Civil and Environmental Engineering, The Hong Kong Polytechnic University, Hung Hom, Kowloon, Hong Kong*

(Received June 11, 2015, Revised September 25, 2015, Accepted October 15, 2015)

Abstract. The Canton Tower is a high-rise slender structure with a height of 610 m. A structural health monitoring system has been instrumented on the structure, by which data is continuously monitored. This paper presents an investigation on the identified modal properties of the Canton Tower using ambient vibration data collected during a whole day (24 hours). A recently developed Fast Bayesian FFT method is utilized for operational modal analysis on the basis of the measured acceleration data. The approach views modal identification as an inference problem where probability is used as a measure for the relative plausibility of outcomes given a model of the structure and measured data. Focusing on the first several modes, the modal properties of this supertall slender structure are identified on non-overlapping time windows during the whole day under normal wind speed. With the identified modal parameters and the associated posterior uncertainty, the distribution of the modal parameters in the future is predicted and assessed. By defining the modal root-mean-square value in terms of the power spectral density of modal force identified, the identified natural frequencies and damping ratios versus the vibration amplitude are investigated with the associated posterior uncertainty considered. Meanwhile, the correlations between modal parameters and temperature, modal parameters and wind speed are studied. For comparison purpose, the frequency domain decomposition (FDD) method is also utilized to identify the modal parameters. The identified results obtained by the Bayesian method, the FDD method and a finite element model are compared and discussed.

Keywords: supertall structure; ambient vibration; modal identification; Bayesian method; uncertainty

1. Introduction

Structural health monitoring (SHM) aims at monitoring existing structures and assessing their service condition. It has attracted increasing attention in the past two decades (Chang *et al*. 2003, Sohn *et al*. 2003, Brownjohn *et al*. 2005, Ko and Ni 2005, Ni *et al*. 2009, Yuen and Kuok 2010, Ni

*Corresponding author, Ph.D., E-mail: yanchunni@gmail.com
[a] Assistant Professor, E-mail: fengliangzhang@hotmail.com
[b] Professor, E-mail: ceyqni@polyu.edu.hk
[c] Ph.D. Student, E-mail: yw.wang@connect.polyu.hk

http://www.techno-press.org/?journal=sss&subpage=8 ISSN: 1738-1584 (Print), 1738-1991 (Online)

et al. 2011, Pei *et al*. 2011, Pei *et al.* 2012, Shi *et al*. 2012, Au *et al*. 2013). Numerous supertall buildings have been erected in recent years worldwide, such as the Canton Tower, the Shanghai Tower, the Shanghai World Financial Center in China. For these large-scale structures, an SHM system is usually instrumented to perform real-time monitoring and provides valuable information for the evaluation of structural performance. Considerable research has been made based on the collected data. Brownjohn and Pan (2008) carried out the analysis of long-term monitoring data from a tall building in terms of loading and response mechanisms. Ni *et al*. (2009, 2011) implemented a sophisticated long-term SHM system on the Canton Tower and collected monitoring data during more than twenty earthquakes and over ten typhoons. Kijewski-Correa *et al*. (2013) presented a real-time SHM system named SmartSync which has been installed on Burj Khalifa ─ the world's tallest building. Su *et al*. (2013) implemented a long-term structural performance monitoring system on the Shanghai Tower. Preliminary monitoring data during different construction stages were presented to evaluate the in-construction condition of the structure.

In SHM systems, accelerometers play an important role in measuring dynamic response of the objective structures (Ni *et al.* 2009, Au *et al*. 2013). Based on the measured acceleration response, operational modal analysis provides an economic way to identify the modal properties, i.e., natural frequency, damping ratio and mode shape, which reflect the dynamic characteristics of the objective structure and are significant for model updating, damage detection, structural health monitoring, etc. (Au and Zhang 2015, Ni *et al*. 2015, Zhang and Au 2015). Au *et al*. (2012b) investigated the modal parameters of two tall buildings during strong wind events by operational modal analysis. Important trends are found between modal parameters and vibration amplitude. Li *et al*. (2011) performed field measurement and numerical analysis of Taipei 101 Tower. The modal parameters were identified based on measured data and compared with finite element model (FEM). Li and Yi (2015) presented their work on the monitoring of dynamic behavior of tall buildings during typhoons. Amplitude-dependent characteristics of damping ratios were identified.

A variety of methods have been developed to perform operational modal analysis. In the time domain, one common method is the stochastic subspace identification (SSI) method (Peeters and De Roeck 2001). The FDD method (Brincker 2001) is another commonly used technique. Besides non-Bayesian methods, a series of Bayesian method have been developed, such as Bayesian Time-Domain Approach (Yuen and Katafygiotis 2001), Bayesian Spectral density Approach (Katafygiotis and Yuen 2001), Bayesian Fourier Transform Approach (Yuen and Katafygiotis 2003), Bayesian modal identification using nonstationary noisy response measurement (Yuen and Katafygiotis 2005). More work can be referred to Yuen (2010).

On the basis of Bayesian Fourier Transform Approach (Yuen and Katafygiotis 2003), the recently proposed Fast Bayesian FFT (Fast Fourier Transform) method (Au 2011, 2012a, b, Au and Zhang 2012a, Zhang and Au 2013) is becoming popular and has been applied in different structures successfully (Au and Zhang 2012b, Au *et al.* 2012a, b, 2013). The approach views modal identification as an inference problem where probability is used as a measure for the relative plausibility of outcomes given a model of the structure and measured data. Using this method, the most probable value (MPV) of modal parameters can be identified. Furthermore, the associated posterior uncertainty of the modal parameters can be calculated analytically without resorting to finite difference, providing an important tool to evaluate the reliability of the identified modal properties.

From the SHM system instrumented on the Canton Tower (Ni *et al.* 2012), 24 hours acceleration, temperature, wind direction and wind speed data were obtained. Based on the Fast

Bayesian FFT method, this paper presents an investigation on the operational modal analysis of this supertall building. Focusing on the first several modes, the modal properties of the Canton Tower are identified on non-overlapping time windows during the whole day under norm wind speed. With the identified modal parameters and the associated posterior uncertainty, the distribution of the modal parameters in the future is assessed by using a probabilistic model. By defining the modal root-mean-square value in terms of the power spectral density (PSD) of modal force identified, the identified natural frequencies and damping ratios versus the vibration amplitude are investigated with the associated posterior uncertainty considered. Meanwhile, the relationships between the modal parameters and temperature, modal parameters and wind speed are investigated. The conventional FDD method is also utilized to identify the modal parameters which will be compared with the results identified by the Fast Bayesian method. The results identified using monitoring data are also compared with those obtained by FEM.

2. Canton Tower

The Canton Tower situated in Guangzhou, China, is a supertall structure with a height of 610 m, as shown in Fig. 1, which serves for emission of television signal, offices, entertainment, sightseeing, etc. This structure is composed of two tube-like structures, namely a reinforced concrete inner structure and a steel outer structure with concrete-filled-tube (CFT) columns. Based on the design drawings, a full-order 3D FEM of the tower has been developed using the commercial software ANSYS with 122,476 elements, 84,370 nodes, and 505,164 degrees-of-freedom (DOFs) in total (Ni *et al.* 2012). To improve the computational efficiency of the model in SHM, a reduced-order 3D model was further developed on the basis of the full model. The modal properties calculated using the two models are consistent with each other and they can be used for comparison with the modal identification results and for model updating.

Fig. 1 Overview of Canton Tower

The SHM system deployed on the Canton Tower consists of more than 700 sensors, including anemometers, accelerometers, fiber optic strain and temperature sensors, global position system, and so on (Ni *et al*. 2009, Chen *et al.* 2011, Ni *et al*. 2012). Among others, 20 uni-axial accelerometers are installed on 8 different cross-sections of the inner structure to collect the structural dynamic responses. On cross-sections 4 and 8, four accelerometers are positioned at two locations for bi-axial measurement; while on each of the other cross-sections, two sensors are installed at two locations for uni-axial measurement (one is for the short-axis direction and the other is for the long-axis direction). The detailed information of the instrumentation can be found in Ni *et al*. (2012). Note that sensors 01, 03, 05, 07, 08, 11, 13, 15, 17, 18 are deployed to collect the structural response in the short-axis direction and sensors 02, 04, 06, 09, 10, 12, 14, 16, 19, 20 measure the structural response in the long-axis direction. Each sensor is aligned using a positioner to ensure an accurate orientation. The frequency range of accelerometers is DC to 50 Hz with amplitude range of ± 2 g. The 24-hour acceleration data used in the present study were collected from 18:00, 20th January 2010 to 18:00, 21st January 2010 under norm wind condition with wind and temperature information recorded simultaneously. The sampling frequencies of wind data, acceleration and temperature are set to be 50 Hz, 50 Hz and 1/60 Hz, respectively.

3. Method for modal analysis

3.1 Fast Bayesian FFT method

In operational modal identification from ambient vibration, the loading and response are usually approximated as stationary stochastic process. For this purpose, the whole 24-hour data are divided into non-overlapping time windows at 30-min intervals. It is found that 30-min time window is appropriate for compromise between the accuracy in modal identification and the stationarity assumption on the stochastic excitation and response. If the data set is too short, the identified modal parameters may have a larger posterior uncertainty and the MPV may be unreliable. Contrarily, when the data set is too long, the stationary assumption cannot be satisfied well, which may increase the modelling error.

The Fast Bayesian FFT method is used to identify the modal properties with each set of data in 30-minute time window. In the traditional operation modal analysis methods, the power spectral density of modal force is usually assumed to be a constant up to the Nyquist frequency. However, this may not be true in reality, especially for the wind loading. In the Fast Bayesian method adopted in this study, it is instead assumed that the PSD of modal force in a selected frequency band is a constant, which makes it possible to analyze the data reasonably. The underlying theory is outlined in the following (Au and Zhang 2012b, Ni *et al*. 2015). Please find the original formulation in Yuen and Katafygiotis (2003) and the recently developed Fast Bayesian FFT algorithms that allow practical implementation in Au (2011), Au (2012a, b) and Zhang and Au (2013).

Let $\boldsymbol{\theta}$ denote the modal parameters which includes modal frequency *f*, damping ratio ζ, mode shapes, power spectral density (PSD) of modal force *S*, and PSD of prediction error S_e. Let $\mathbf{Z}_k = [\mathrm{Re}\mathcal{F}_k; \mathrm{Im}\mathcal{F}_k] \in R^{2n}$ be an augmented vector of the real and imaginary parts of $\mathcal{F}_k$, where $\mathcal{F}_k$ denotes the FFT of the measured response at frequency f_k, and *n* is the number of measured

degrees of freedom (DOFs). In modal identification, only the FFT data confined to a selected frequency band dominated by the target modes are used, which is denoted by $\{\mathbf{Z}_k\}$. On the basis of Bayes' Theorem, the posterior probability density function (PDF) of $\boldsymbol{\theta}$ given the data in the band is expressed by

$$p(\boldsymbol{\theta}|\{\mathbf{Z}_k\}) \propto p(\boldsymbol{\theta})p(\{\mathbf{Z}_k\}|\boldsymbol{\theta}) \tag{1}$$

where $p(\boldsymbol{\theta})$ is the prior PDF that reflects the plausibility of $\boldsymbol{\theta}$ in the absence of data. Assuming uniform prior information, the posterior PDF $p(\boldsymbol{\theta}|\{\mathbf{Z}_k\})$ is directly proportional to the likelihood function $p(\{\mathbf{Z}_k\}|\boldsymbol{\theta})$. The most probable value (MPV) of the modal parameters $\boldsymbol{\theta}$ can be determined by maximizing $p(\boldsymbol{\theta}|\{\mathbf{Z}_k\})$ and hence $p(\{\mathbf{Z}_k\}|\boldsymbol{\theta})$.

For a large number of sampling points and a small time interval, the FFT at different frequencies is shown to be asymptotically independent and follow a Gaussian distribution (Schoukens 1991), based on which the likelihood function $p(\{\mathbf{Z}_k\}|\boldsymbol{\theta})$ can be given by

$$p(\{\mathbf{Z}_k\}|\boldsymbol{\theta}) = \prod_k (2\pi)^{-n} (\det \mathbf{C}_k)^{-1/2} \exp[-\frac{1}{2}\mathbf{Z}_k^T \mathbf{C}_k^{-1} \mathbf{Z}_k] \tag{2}$$

where $\det(.)$ denotes the determinant; $\mathbf{C}_k$ denotes the covariance matrix of $\mathbf{Z}_k$, in which the modal parameters to be identified are involved.

For the convenience of optimization, the negative log-likelihood function (NLLF) $L(\boldsymbol{\theta})$ is utilized

$$L(\boldsymbol{\theta}) = \frac{1}{2}\sum_k [\ln \det \mathbf{C}_k(\boldsymbol{\theta}) + \mathbf{Z}_k{}^T \mathbf{C}_k(\boldsymbol{\theta})^{-1} \mathbf{Z}_k] \tag{3}$$

so that

$$p(\boldsymbol{\theta}|\{\mathbf{Z}_k\}) \propto \exp[-L(\boldsymbol{\theta})] \tag{4}$$

Therefore, minimizing $L(\boldsymbol{\theta})$ with respect to $\boldsymbol{\theta}$ is equivalent to maximizing $p(\boldsymbol{\theta}|\{\mathbf{Z}_k\})$.

When performing optimization to obtain the MPV of $\boldsymbol{\theta}$, the minimization process is ill-conditioned. Furthermore, the number of modal parameters will increase with the number of measured DOFs, and so the computational time grows drastically with the number of parameters to be optimized. Therefore, it is highly desirable to develop fast algorithms in real applications. This has been realized recently which allows the MPV to be obtained almost instantaneously in both cases of well separated modes (Au 2011, Zhang and Au 2013) and closely-spaced modes (Au 2012a,b). Meanwhile, the posterior uncertainty can also be obtained directly to assess the accuracy of the MPV and evaluate whether additional data is required for quality improvement. In modal identification by the proposed method, a frequency band should be selected in either separated or closely-spaced mode case. In recognition of the limited bandwidth in physical processes and the

fact that the resonance band accounts for the major contribution, the root-mean-square (RMS) value of the acceleration response can be calculated according to Au *et al.* (2012), which can be used to represent the vibration level of a given mode.

3.2 Prediction model

With the Fast Bayesian FFT method, the MPV of modal parameters and the associated posterior uncertainty can be determined. After obtaining them, a probabilistic model can be obtained as follows (Zhang and Au 2015)

$$p_{\Theta}(\theta \mid D) = \frac{1}{N_s} \sum_{i=1}^{N_S} \frac{1}{\sqrt{2\pi \hat{c}_i}} \exp\left[-\frac{1}{2\hat{c}_i} (\theta - \hat{\theta}_i)^2 \right] \tag{5}$$

which is a mixture of Gaussian PDFs, where N_s denotes the number of data sets; $\hat{c}$ is the posterior variance of the identified modal parameters; $\hat{\theta}_i$ is the posterior MPV of θ with θ being a particular parameter in $\boldsymbol{\theta}$, D denotes the data involved. With Eq. (5), we can obtain the mean and variance.

Combining both Bayesian and frequentist features, the proposed method is able to assess the modal parameters in a future time window with the monitoring data acquired at the next time interval, and therefore provides a novel way to make a prediction to the distribution of modal properties of an objective structure in a similar excitation environment.

4. Analysis results

4.1 Typical 30-min window

As aforementioned, the 24-hour data were separated into 48 time windows of 30 minutes each. The analysis for the first time window of data is pursued and the same procedure is applied to other time windows. Fig. 2 shows the root power spectral density spectra of the structural responses during a typical time window. Fifteen peaks are obviously observed in the frequency range below 2.0 Hz. The first mode is less than 0.1 Hz, which is the foundational mode of the Canton Tower. In the operational modal analysis by the Fast Bayesian FFT method, all the fifteen modes are explored.

Table 1 shows the identified modal parameters of the fifteen modes. From the second to the ninth columns, every two columns are considered as one group with the first denoting the MPV and the second denoting the associated posterior coefficient of variation (COV) (standard derivation/MPV). It is seen that the COVs of modal frequencies are quite small (less than 0.5%), implying that the MPVs are quite accurate. The damping ratios for this structure are quite small and only those of the first and fourth modes are higher than 1%. This is consistent with the results obtained by Chen *et al.* (2011) for the same structure under ambient vibration condition. The posterior uncertainty of damping ratios is relatively high in comparison with the uncertainty of modal frequencies, with an order of magnitude of a few tens percent. The other two parameters, i.e., PSD of modal force and PSD of prediction error, are related to the excitation environment. The COV of the PSD of modal force is apparently larger than the COV of the PSD of prediction error.

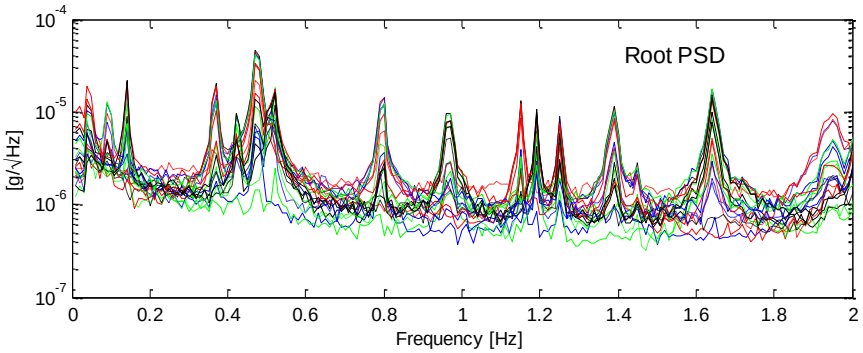

Fig. 2 Power spectral density for a typical 30-min window

Table 1 Identified modal parameters and the associated posterior uncertainty

Mode	Characteristics	f (Hz)	COV (%)	ζ (%)	COV (%)	S (μg^2/Hz)	COV (%)	S_e (μg^2/Hz)	COV (%)
1	Bending	0.094	0.37	1.20	32.5	1.64	17.5	5.56	3.21
2	Bending	0.138	0.18	0.48	39.9	0.92	17.3	3.49	3.50
3	Bending	0.366	0.08	0.26	32.5	0.30	10.9	1.49	2.28
4	Bending	0.424	0.07	0.21	35.7	0.05	17.1	2.25	3.28
5	Bending	0.475	0.05	0.12	41.6	0.88	11.8	1.77	2.58
6	Torsion	0.506	0.04	0.10	46.4	0.05	21.5	8.83	4.00
7	Bending	0.522	0.07	0.27	29.1	0.19	15.6	2.52	3.01
8	Bending	0.796	0.05	0.23	23.2	0.08	7.8	0.81	1.61
9	Bending	0.966	0.06	0.36	17.5	0.06	7.6	0.65	1.50
10	Combined	1.151	0.03	0.13	26.8	0.01	11.7	0.63	2.35
11	Bending	1.191	0.03	0.11	29.1	0.01	12.9	0.84	2.53
12	Torsion	1.250	0.03	0.11	27.6	0.01	9.8	0.66	1.94
13	Bending	1.388	0.05	0.33	16.0	0.05	8.4	0.50	1.63
14	Bending	1.643	0.04	0.22	16.7	0.07	6.4	0.51	1.33
15	Combined	1.946	0.08	0.74	11.6	0.09	10.3	0.62	1.53

f: Modal frequency; ζ :damping ratio; S: PSD of modal force; S_e: PSD of prediction error

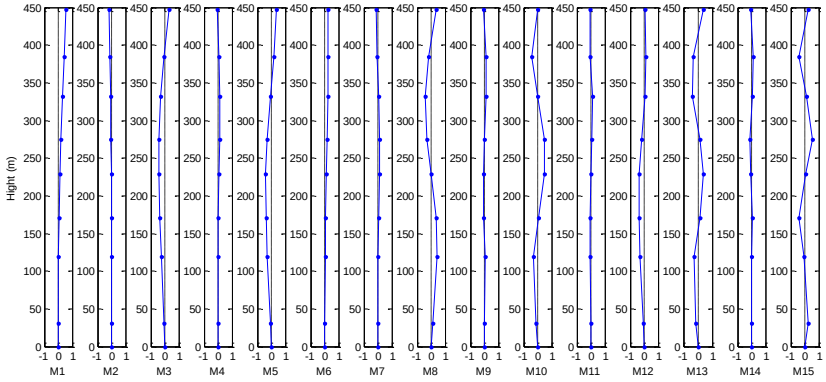

Fig. 3 Identified mode shapes for the first 15 modes projected in short-axis direction

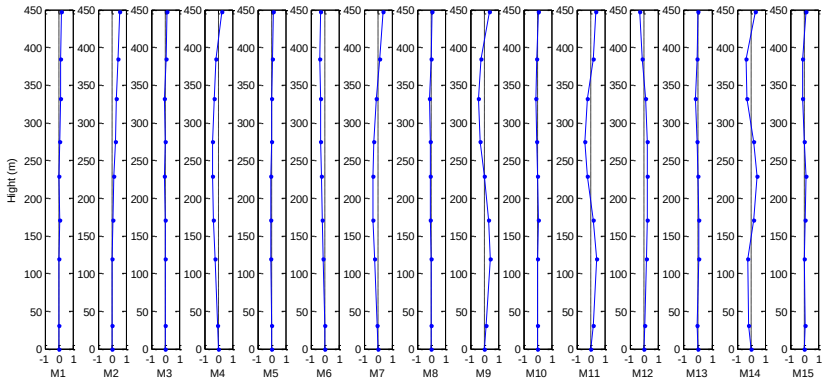

Fig. 4 Identified mode shapes for the first 15 modes projected in long-axis direction

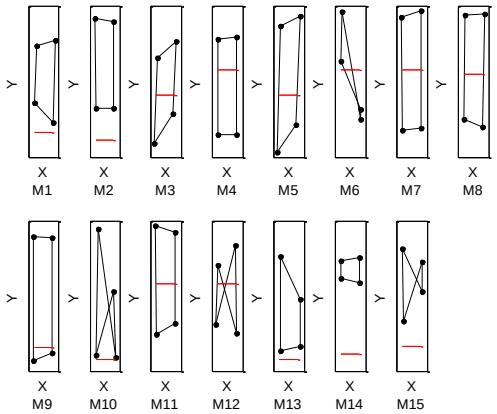

Fig. 5 XY view of identified mode components on cross-sections 4 and 8

Figs. 3 and 4 illustrate the identified mode shapes of the fifteen modes projected in short- and long-axis directions, respectively. In each mode shape, eight locations in different cross-sections with uni-axial measurement are chosen. As afore mentioned, four accelerometers have been deployed for bi-axial measurement at two plane locations on cross-sections 4 and 8. This makes it possible to investigate the torsional behavior of these modes. Fig. 5 shows the top view (XY view) of the identified mode components at these four locations on two different cross-sections, where the red and black lines denote the undeformed and deformed status, respectively. It is observed that although the mode shapes for some modes shown in Figs. 3 and 4 are similar when projected in short- or long-axis direction, they are different in top view, where Modes 6, 10, 12, 15 exhibit a significant torsional behavior.

To verify the results identified by the Fast Bayesian FFT method, the enhanced FDD method is utilized to identify the modal parameters as well. Table 2 shows the modal frequencies and damping ratios identified by the enhanced FDD method. It is seen that the identified modal frequencies for different modes are quite consistent with their counterparts determined by the Fast Bayesian FFT method. However, it is not true for the damping ratios, where a noticeable difference is observed between the two groups of results. This implies that high uncertainty exists in the identified damping ratios, as evidenced by the large posterior COVs of damping ratios obtained by the Fast Bayesian FFT method.

Table 2 Modal parameters identified by enhanced FDD method

Mode	Modal frequency (Hz)	Damping ratio (%)
1	0.094	2.48
2	0.138	1.33
3	0.366	0.46
4	0.424	0.32
5	0.475	0.29
6	0.506	0.28
7	0.522	0.43
8	0.796	0.46
9	0.965	0.64
10	1.151	0.16
11	1.191	0.16
12	1.250	0.16
13	1.390	0.34
14	1.642	0.27
15	1.948	0.86

Table 3 Modal parameters predicted by FEM

Mode	Modal frequency (Hz)	
	Full model	Reduced model
1	0.110	0.110
2	0.159	0.159
3	0.347	0.347
4	0.368	0.368
5	0.400	0.399
6	0.461	0.460
7	0.485	0.485
8	0.738	0.738
9	0.902	0.902
10	0.997	0.997
11	1.038	1.038
12	1.122	1.122
13	1.244	1.244
14	1.503	1.503
15	1.726	1.726

Table 3 shows the modal parameters for the first 15 modes predicted by the FEM. It is found that the results from the full- and reduced-order models are well consistent with each other. Compared with the identified results using the Fast Bayesian FFT method, it is seen that they are in general close to the results by the FEM but some obvious difference is also observed. This is reasonable since the FEM is formulated based on the design drawings, and some alterations have been made from the design to construction stages. Mode shapes also play an important part in investigating the quality of FEM by comparing them with their counterparts in the identified results (Chen *et al*. 2012). It is necessary to obtain an accurate FEM by model updating based on the field data (Chen and Huang 2012, Kuok and Yuen 2012, Lei *et al.* 2012). A new developed Bayesian method (Au and Zhang 2015, Zhang and Au 2015) is also expected to perform model updating in the future.

Based on these data, some researches have been carried out in a special issue on SHM Benchmark for High-Rise Structures in the Smart Structures and Systems, Vol. 10, No. 4-5, including modal identification based on Bayesian spectral density approach (BSDA) (Kuok and Yuen 2012), Vector Autoregressive Models (ARV) method (Niu *et al.* 2012) and so on. Table 4 shows the identified results for the first ten modes using BSDA and ARV methods. In the BSDA method, similar to the results identified by Fast Bayesian FFT method, the posterior COV values

of natural frequencies and damping ratios are also calculated. In the ARV method, the COV values are equal to the sample standard derivation divided by the sample means. Compared the results in Table 1, Table 2 and Table 4, it is seen that the natural frequencies across different methods are quite similar while there are some variation for the damping ratio. This is reasonable since the damping ratios have a relatively larger uncertainty. Compared the posterior COVs obtained by BSDA and Fast Bayesian FFT method, it is seen that they have similar order of magnitudes, showing a good consistency. The sample COVs calculated by ARV method in Table 4 tend to be larger than those by the Bayesian method. This is reasonable since modal parameters variations among different data sets are taken into account when calculating the sample COVs.

4.2 Variation of modal parameters in a period of 24 hours

We next investigate the variation of modal parameters with environmental conditions in one day. Fig. 6 shows the 10-min averaged wind speed, wind direction and temperature measured by the sensors installed on the tower during the same day. It is seen that the wind speed is relatively stable with a fluctuation from about 1.5 to 4 m/s and there is no much change for the wind direction, while the temperature changes from 14 to 18^{o}C gradually. Overall, the environment is relatively stationary during the 24 hours. The 48 segments of acceleration data are analyzed separately with the procedure described in Section 4.1. In this study, only the first three modes are addressed.

Fig. 7 to Fig. 9 show the modal parameters identified using the 48 sets of data and the associated uncertainty for Modes 1 to 3, respectively. The identified results for each dataset are shown with a dot at the posterior MPV and an error bar covering two posterior standard deviations. It is seen that the modal frequencies of the three modes change slightly with time, while the damping ratios have a relatively large variation but still have the same order of magnitude. The posterior uncertainty is consistent with the ensemble variability of their MPVs over different setups and therefore the Bayesian and frequentist perspectives roughly agree.

Table 4 Modal parameters identified by BSDA (Kuok and Yuen 2012) and ARV (Niu *et al.* 2012)

Method		M1	M2	M3	M4	M5	M6	M7	M8	M9	M10
BSDA	f(Hz)	0.095	0.140	0.368	0.426	0.477	0.507	0.524	0.797	0.967	1.152
	COV(%)	0.24	0.12	0.07	0.06	0.04	0.05	0.05	0.04	0.03	0.02
	ζ (%)	1.03	0.50	0.35	0.25	0.19	0.16	0.14	0.20	0.19	0.11
	COV(%)	22.7	21.1	20.2	24.3	20.3	38.4	30.9	18.3	16.3	21.6
ARV	f(Hz)	0.094	0.138	0.366	0.424	0.475	0.506	0.522	0.795	0.965	1.151
	COV(%)	0.30	0.21	0.21	0.08	0.07	0.11	0.08	0.13	0.15	0.05
	ζ (%)	0.68	0.39	0.34	0.2	0.12	0.17	0.19	0.26	0.27	0.13
	COV(%)	72.3	51.0	47.2	35.2	86.6	30.3	49.5	78.0	40.1	46.1

On the other hand, a sudden change of modal parameters shall reflect the quality of the data used. Take the data acquired at 16:30 for example. It is seen that the posterior uncertainty of modal frequency and damping ratio for the second mode are larger than other ones. To look for the reason, the time history of the data is shown in Fig. 10, where some strange peaks are observed. These peaks could come from sensor noise, electric noise or some noise in the environment, which affect the stationary assumption of the excitation and thus lead to the inaccuracy of the identified result (say, higher uncertainty). For this kind of data, a recently developed method is expected to perform outlier detection and robust structural identification (Yuen and Mu 2012, Mu and Yuen 2015). This may be investigated in the future work.

Table 5 shows the frequentist and Bayesian statistics for Modes 1 to 3, in which sample COV (sample standard derivation/sample mean) is calculated based on all the 48 datasets, while the posterior COV is the one from the first dataset. These two quantities are quite close to each other, showing good consistency between the frequentist result and the posterior uncertainty of these modal parameters in a Bayesian manner. As aforementioned, since some environmental uncertainties are also taken into account in the sample COV, the posterior COV tends to be smaller than the sample COV. Some relationship has been observed between these two concepts (Au 2012c).

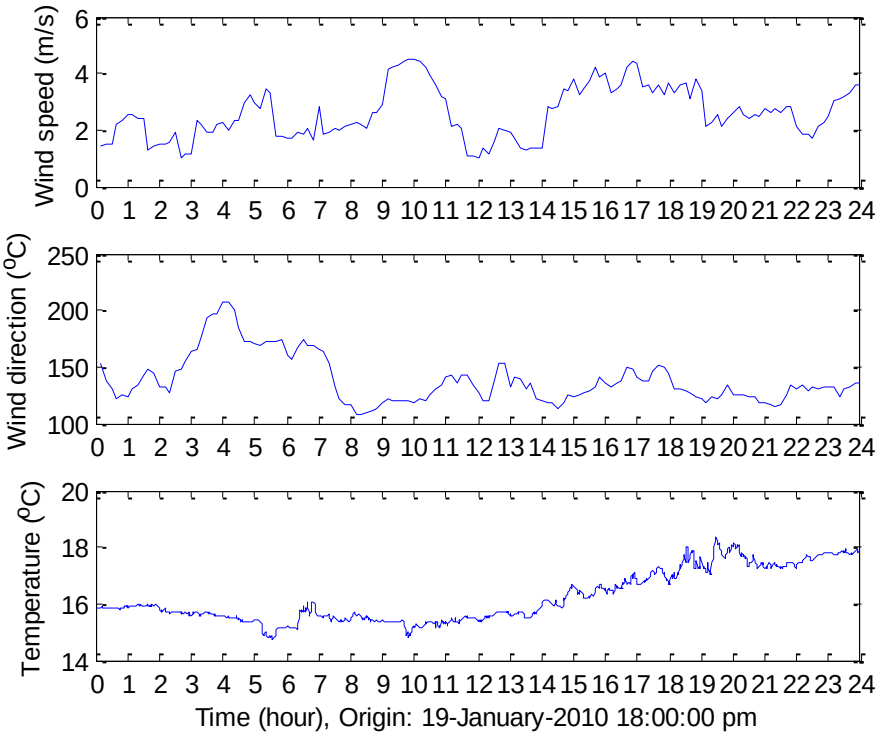

Fig. 6 Wind and temperature data collected during the same day

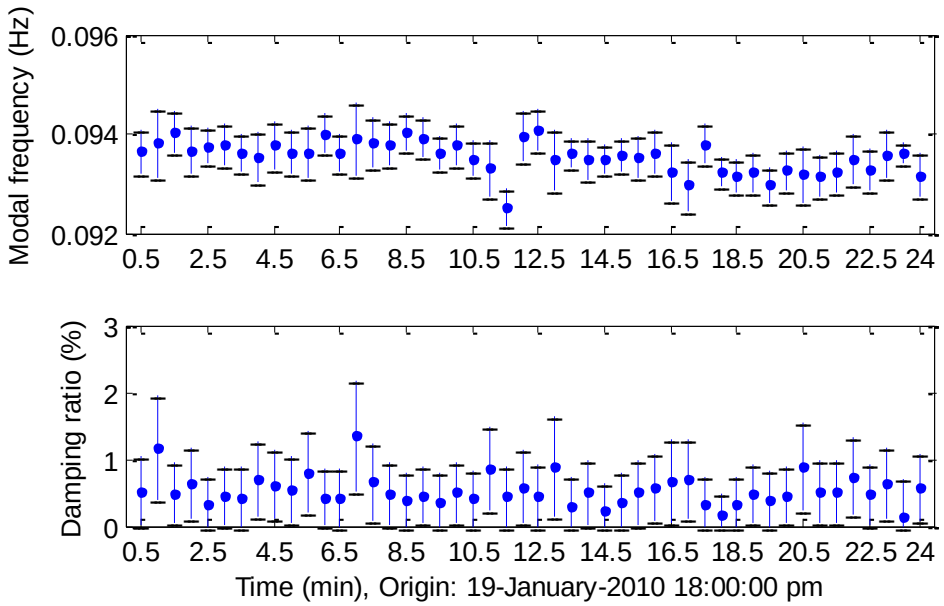

Fig. 7 Modal parameters in different setups, Mode 1

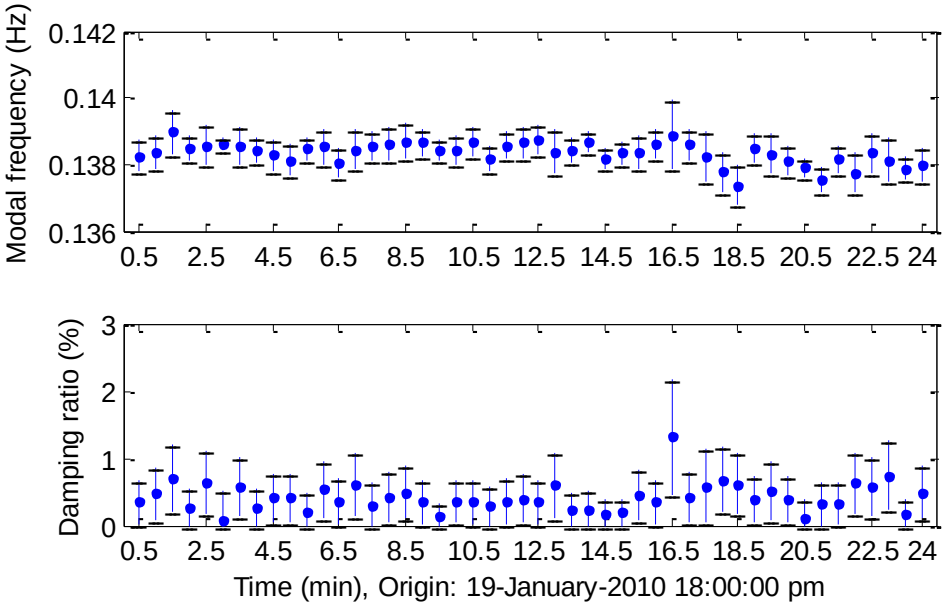

Fig. 8 Modal parameters in different setups, Mode 2

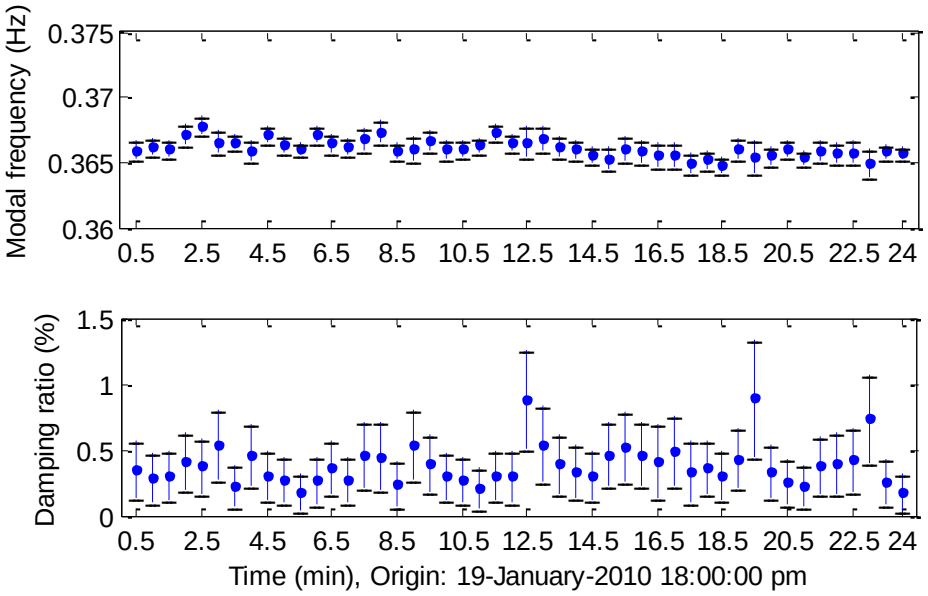

Fig. 9 Modal parameters in different setups, Mode 3

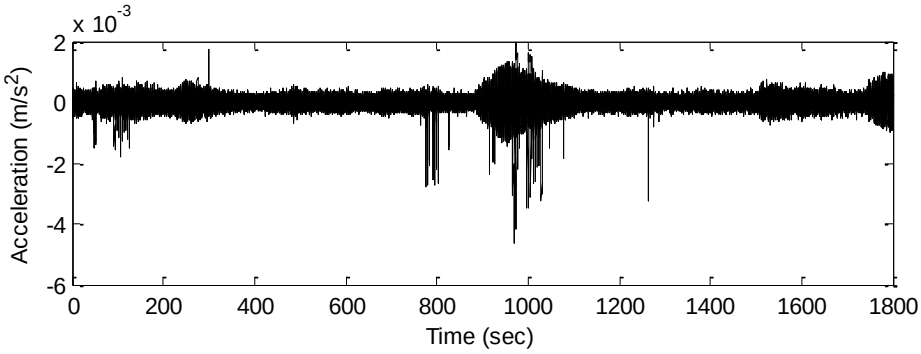

Fig. 10 Time history of acceleration response acquired at 16:30

Table 5 Sample COVs and posterior COVs

Mode	Modal frequency (%)		Damping ratio (%)	
	Posterior COV	Sample COV	Posterior COV	Sample COV
1	0.24	0.35	48.9	42.1
2	0.16	0.24	46.5	49.9
3	0.10	0.18	30.6	39.7

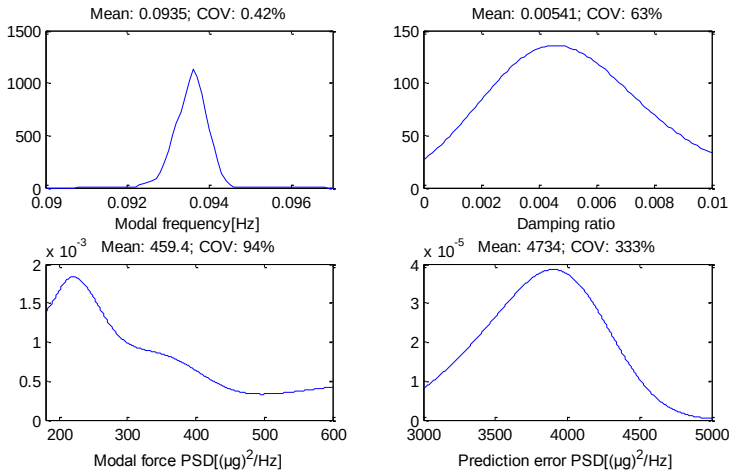

Fig. 11 PDF of modal parameters derived from probabilistic model, Mode 2

Fig. 11 to Fig. 13 show the probability density functions of the modal parameters in a future scenario incorporating the information from the 48 datasets in accordance with the probabilistic model derived for Modes 1 to 3, respectively. In this case, the distributions for the modal frequency, damping ratio and PSD of prediction error are approximated to be Gaussian while for the PSD of modal force, the distribution is quite different. This is also attributed to that the PSD of modal force is easier to be influenced by the environment as mentioned. In these three figures, the mean and COV of the distribution are shown above each subfigure. It is found that the posterior COVs in a single setup tend to be smaller than those calculated based on the probabilistic model. This indicates that the posterior uncertainty represented by the prediction model is higher than the posterior uncertainty of a single dataset, which may be attributed to that in the former case, the data variability among different datasets is taken into account, but not for the latter case.

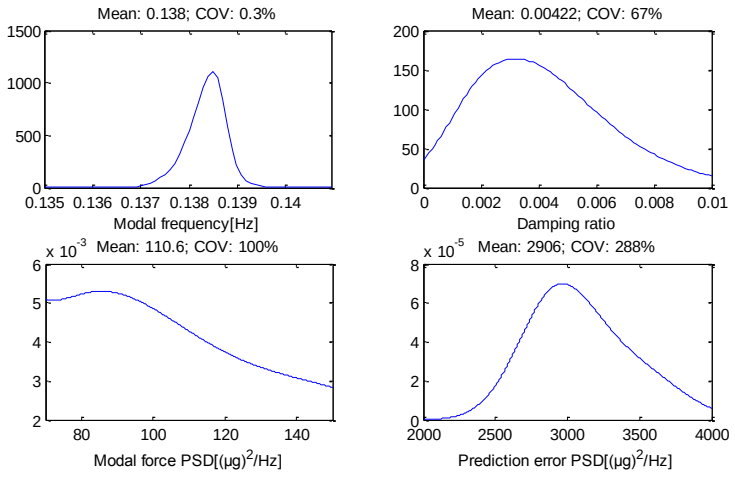

Fig. 12 PDF of modal parameters derived from probabilistic model, Mode 2

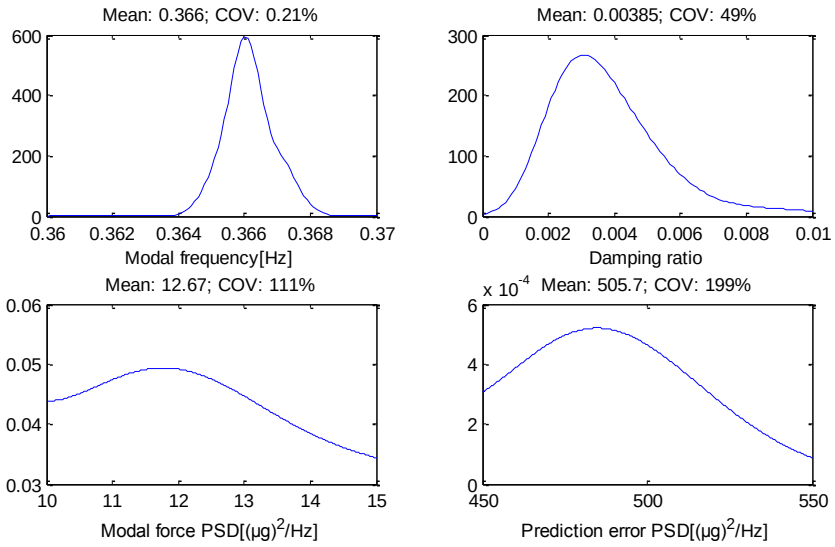

Fig. 13 PDF of modal parameters derived from probabilistic model, Mode 3

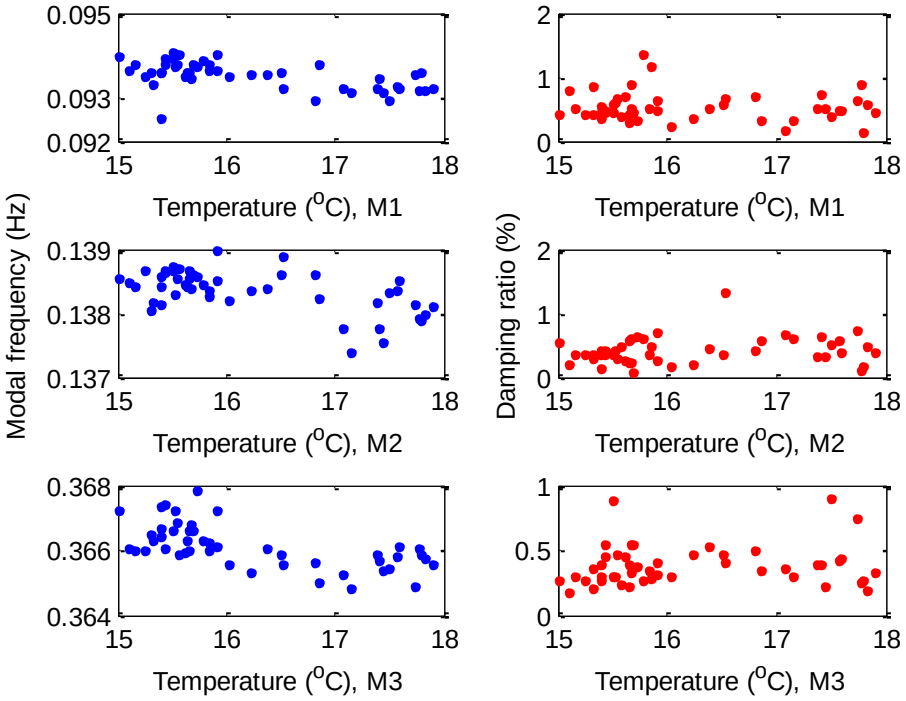

Fig. 14 Modal parameters identified from different datasets versus temperature

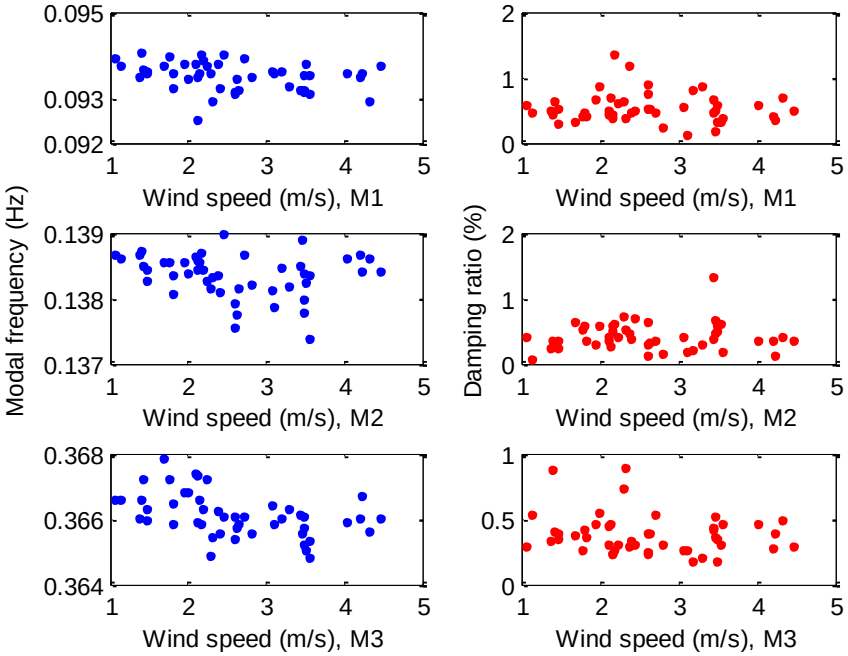

Fig. 15 Modal parameters identified from different datasets versus wind speed

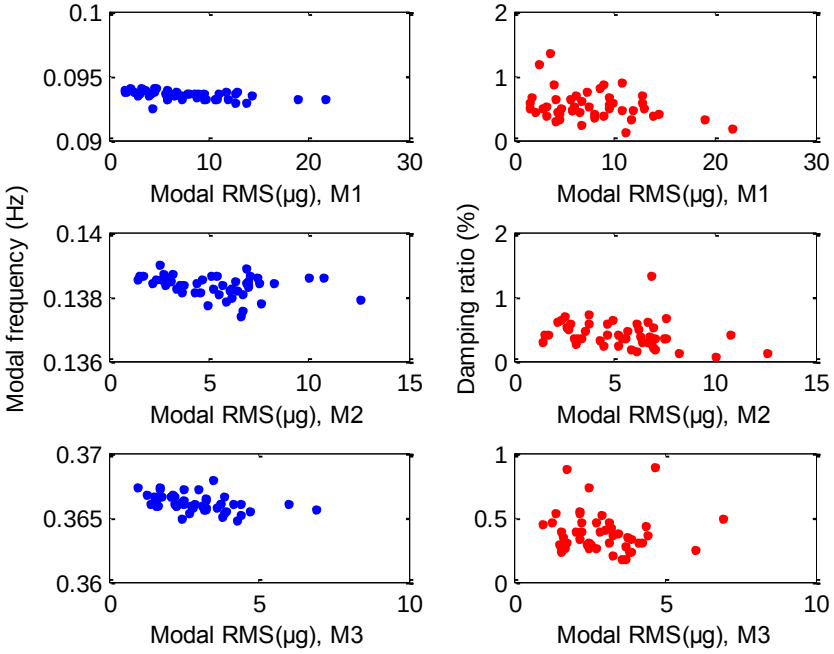

Fig. 16 Modal parameters versus vibration amplitude

From Fig. 7 to Fig. 9, it is difficult to find the correlation between the modal parameters and wind speed, modal parameters and temperature. Figs. 14 and 15 show the modal parameters identified from different datasets versus the temperature and wind speed, respectively. It is seen that there is slightly descending trend for the modal frequencies with the increase of temperature. A similar trend is also observed in the correlation between the modal frequencies and wind speed, although it is even not obvious. The trend for the damping ratios is difficult to identify since the changes of temperature and wind speed in a normal day are too slight, and the amplitude-dependent characteristics are not obvious.

Using the Fast Bayesian FFT method, one important merit is that the PSD of modal force can be identified directly. This makes it possible to estimate the modal root mean square (RMS) value of the *i*th mode according to the following equation (Au *et al.* 2012b)

$$RMS_i = \frac{\pi f_i S_i}{4\zeta_i} \tag{6}$$

where f_i, ζ_i, and S_i denotes the modal frequency, damping ratio and PSD of modal force of the *i*th mode, respectively. The RMS value of the modal response in a given time window is utilized to represent the vibration level in a given mode.

Fig. 16 shows the relationship between the modal frequency and modal RMS, the damping ratio and modal RMS for Modes 1 to 3. The modal frequency decreases with the increase of vibration level for each mode. This result is consistent with the investigation in Au et al. (2012b), where two tall buildings were studied under strong winds. Similar to Figs. 14 and 15, there is no obvious trend for the damping ratio. To examine the rationality of the definition of modal RMS, the relationship between wind speed and modal RMS for Modes 1 to 3 is plotted in Fig. 17. It is seen that the modal RMS increases with wind speed in an approximately linear manner for each mode, implying that the wind speed has an evident correlation with the modal RMS. This is consistent with our intuition.

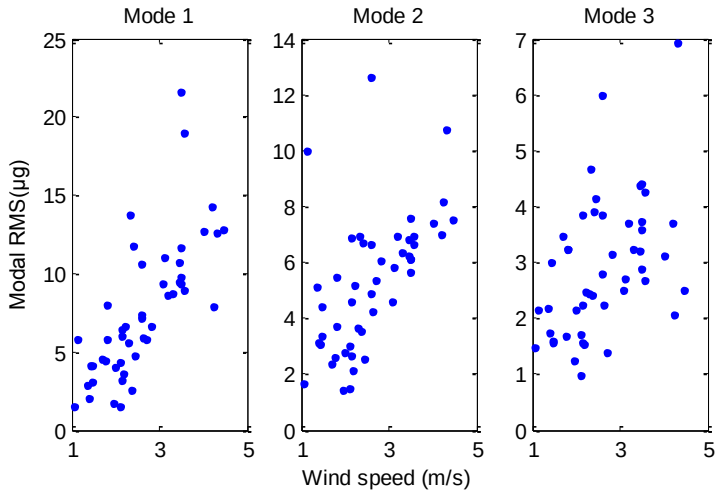

Fig. 17 Wind speed versus vibration amplitude

5. Conclusions

This paper presents the work on operational modal analysis of the Canton Tower using the recently developed Fast Bayesian FFT method. In addition to the most probable value of modal parameters, the method also makes it possible to evaluate the associated posterior uncertainty analytically. The modal parameters of fifteen modes are identified, including the modal frequency, damping ratio, mode shape, modal force PSD and prediction error PSD. The modal frequency of the first mode is very low (less than 0.1 Hz), and it is consistent with the properties of this supertall structure. The identified damping ratios for all the modes are relatively small under ambient excitation conditions. The identification of modal frequencies is more accurate than that of damping ratios with a small posterior uncertainty for the former. It is interesting to find that the mode shapes of some modes are similar in translational direction and the main difference is reflected in their torsional behaviors. The identified modal frequencies obtained by the Fast Bayesian FFT method are consistent with those identified by the enhanced FDD method, BSDA and ARV method, while some differences exist for the damping ratio. By comparing the identified results and those obtained from FEM, certain variation is observed for some modal frequencies. It is necessary to perform model updating in the future.

Based on the acceleration, wind speed, wind direction and temperature data collected in a whole day, 48 sets of modal parameters are identified to investigate the relationship with the wind speed, temperature and modal RMS of the acceleration response. By plotting the MPV and the associated posterior uncertainty of all the identified results together, the data with outlier can be detected by comparing the posterior uncertainty of modal parameters and checking their consistency. It is also seen that the modal frequencies have a slightly descending trend with the temperature, wind speed and modal vibration amplitude, while this is not true for the damping ratios under ambient excitation conditions. Furthermore, by comparing the correlation between the modal RMS and the wind speed, an approximately linear relationship between these two quantities is found, implying that the definition of the modal RMS in terms of the PSD of modal force is reasonable.

The posterior uncertainties in the frequentist and Bayesian perspectives are consistent with each other, although the former tends to be larger than the latter. Based on the modal parameters and the associated posterior uncertainty obtained using the non-overlapping datasets, the distribution of the modal parameters in a future time window is predicted and assessed. It is found that the distributions of modal frequency, damping ratio and PSD of prediction error are approximately Gaussian, while this is not true for the PSD of modal force due to its dependence on environmental variation.

Acknowledgements

The work described in this paper was supported partially by National Natural Science Foundation of China (Grant Nos.: 51508407, 51508413), partially by a grant from the Shenzhen Science and Technology Innovation Commission (Project No. JC201105201141A), in part by Fundamental Research Funds for the Central Universities, China (Grant No. 2014KJ040) and Shanghai Pujiang Program (Grant No.: 15PJ1408600). The financial support is greatly acknowledged.

References

Au, S.K. (2011), "Fast Bayesian FFT method for ambient modal identification with separated modes", *J. Eng. Mech. - ASCE*, **137**, 214-226.
Au, S.K. (2012a), "Fast Bayesian ambient modal identification in the frequency domain, Part I: Posterior most probable value", *Mech. Syst. Signal Pr.*, **26**, 60-75.
Au, S.K. (2012b), "Fast Bayesian ambient modal identification in the frequency domain, Part II: posterior uncertainty", *Mech. Syst. Signal Pr.*, **26**, 76-90.
Au, S.K. (2012c), "Connecting Bayesian and frequentist quantification of parameter uncertainty in system identification", *Mech. Syst. Signal Pr.*, **29**, 328-342.
Au S.K. and Zhang F.L. (2012a), "Fast Bayesian ambient modal identification incorporating multiple setups", *J. Eng.Mech.* - ASCE, **138**(7), 800-815.
Au, S.K. and Zhang, F.L. (2012b), "Ambient modal identification of a primary-secondary structure by Fast Bayesian FFT method", *Mech. Syst. Signal Pr.*, **28**, 280-296.
Au, S.K. and Zhang, F.L. (2016), "Fundamental two-stage formulation for Bayesian system identification, Part I: General theory", *Mech. Syst. Signal Pr.*, **66-67**, 31-42.
Au, S.K., Ni, Y.C., Zhang, F.L. and Lam, H.F. (2012a), "Full scale dynamic testing of a coupled slab system", *Eng. Struct.*, **37**, 167-178.
Au, S.K., Zhang, F.L. and To, P. (2012b), "Field observations on modal properties of two tall buildings under strong wind", *J. Wind Eng. Ind. Aerod.*, **101**, 12-23.
Au, S.K., Zhang, F.L. and Ni, Y.C. (2013), "Bayesian operational modal analysis: theory, computation, practice", *Comput. Struct.*, **126**, 3-15.
Brincker, R., Zhang, L. and Anderson, P. (2001), "Modal identification of output-only systems using frequency domain decomposition", *Smart Mater. Struct.*, **10**, 441-455.
Brownjohn, J.M.W. and Pan, T.C. (2008), "Identifying loading and response mechanisms from ten years of performance monitoring of a tall building", *J. Perform. Constr. Fac.*, **22**(1), 24-34.
Brownjohn, J.M.W., Moyo, P., Omenzetter, P. and Chakraborty, S. (2005), "Lessons from monitoring the performance of highway bridge", *Struct. Control Health Monit.*, **12**, 227-244.
Chang, P.C., Flatau, A. and Liu, S.C. (2003), "Health monitoring of civil infrastructure", *Struct. Health Monit.*, **2**(3), 257-267.
Chen, H.P., Tee, K.F. and Ni, Y.Q. (2012), "Mode shape expansion with consideration of analytical modelling errors and modal measurement uncertainty", *Smart Struct. Syst.*, **10**(4-5), 485-499.
Chen, H.P. and Huang, T.L. (2012), "Updating finite element model using dynamic perturbation method and regularization algorithm", *Smart Struct. Syst.*, **10**(4-5), 427-442.
Chen, W.H., Lu, Z.R., Lin, W., Chen, S.H., Ni, Y.Q., Xia, Y. and Liao W.Y. (2011), "Theoretical and experimental modal analysis of the Guangzhou New TV Tower", *Eng. Struct.*, **33**, 3628-3646.
Katafygiotis, L.S. and Yuen, K.V. (2001), "Bayesian spectral density approach for modal updating using ambient data", *Earthq. Eng. Struct. D.*, **30**, 1103-1123.
Kijewski-Correa, T., Kwon D.K., Kareem A., Bentz A., Guo Y., Bobby A. and Abdelrazaq, A. (2013), "SmartSync: An integrated real-time structural health monitoring and structural identification system for tall buildings", *J. Struct. Eng.* - ASCE, **139**(10), 1675-1687.
Ko, J.M. and Ni, Y.Q. (2005), "Technology developments in structural health monitoring of large-scale bridges", *Eng. Struct.*, **27**(12), 1715-1725.
Kuok, S.C. and Yuen, K.V. (2012), "Structural health monitoring of Canton tower using Bayesian framework", *Smart Struct. Syst.*, **10**(4-5), 375-391.
Lam, H.F., Peng, H.Y. and Au, S.K. (2014), "Development of a practical algorithm for Bayesian model updating of a coupled slab system utilizing field test data", *Eng. Struct.*, **79**, 182-194.
Lei, Y., Wang, H.F. and Shen, W.A. (2012), "Update the finite element model of Canton Tower based on direct matrix updating with incomplete modal data", *Smart Struct. Syst.*, **10**(4-5), 471-483.

Li, Q.S. and Yi, J. (2015), "Monitoring of dynamic behaviour of super-tall buildings during typhoons", *Struct. Infrastruct. E.*, DOI: 10.1080/15732479.2015.1010223.

Li, Q.S., Zhi, L.H., Tuan, A.Y., Kao, C.S., Su, S.C. and Wu, C.F. (2011), "Dynamic behavior of Taipei 101 Tower: Field measurement and numerical analysis", *J. Struct. Eng. - ASCE*, **137**(1), 143-155.

Mu, H.Q. and Yuen, K.V. (2015), "Novel outlier-resistant extended Kalman filter for robust online structural identification", *J. Eng. Mech. - ASCE*, **141**(1), CID: 04014100.

Ni, Y.Q., Wong, K.Y. and Xia Y. (2011). "Health checks through landmark bridges to sky-high structures", *Adv. Struct. Eng.*, **14**(1), 103-119.

Ni, Y.Q., Xia, Y., Lin, W., Chen, W.H. and Ko, J.M. (2012), "SHM benchmark for high-rise structures: a reduced-order finite element model and field measurement data", *Smart Struct. Syst.*, **10**(4), 411-426.

Ni, Y.Q., Xia, Y., Liao, W.X. and Ko, J.M. (2009), "Technology innovation in developing the structural health monitoring system for Guangzhou New TV Tower", *Struct. Control Health Monit.*, **16**(1), 73-98.

Ni, Y.Q., Zhang, F.L., Xia, Y.X. and Au, S.K. (2015), "Operational modal analysis of a long-span suspension bridge under different earthquake events", *Earthq. Struct.*, **8**(4), 859-887.

Niu Y., Kraemer P. and Fritzen C.P. (2012), "Operational modal analysis for Canton Tower", *Smart Struct. Syst.*, **10**(4-5), 393-410.

Pei, H.F., Cui, P., Yin, J.H, Zhu, H.H., Chen, X.Q., Pei, L.Z. and Xu, D.S. (2011). "Monitoring and warning of landslides and debris flows using an optical fiber sensor technology", *J. Mountain Sci*., **8**(5), 728-738.

Pei, H.F., Yin, J.H., Zhu, H.H, Hong, C.Y., Jin, W. and Xu, D.S. (2012), "Monitoring of lateral displacements of a slope using a series of special fibre Bragg grating-based in-place inclinometers", *Measurement Sci. Technol.*, **23**(2), 1-8.

Peeters, B. and De Roeck, G. (2001), "Stochastic system identification for operational modal analysis: a review". *Journal of Dynamic Systems*", *Measurement Control*, ASME, **123**(4), 659-667.

Schoukens, J. and Pintelon, R. (1991), *Identification of Linear Systems: A Practical Guideline for Accurate Modelling*, London: Pergamon Press.

Shi, W.X., Shan J.Z. and Lu, X.L. (2012), "Modal identification of Shanghai World Financial Center both from free and ambient vibration response", *Eng. Struct.*, **36**, 14-26

Sohn, H., Farrar, C.R., Hemez, F.M., Shunk, D.D., Stinemates, D.W. and Nadler B.R. (2003), *A Review of Structural Health Monitoring Literature: 1996-2001*, Los Alamos National Laboratory Report, LA-13976-MS.

Su, J.Z., Xia, Y., Chen, L., Zhao, X., Zhang, Q.L., Xu, Y.L., Ding, J.M., Xiong, H.B. and Ma, R.J. (2013), "Long-term structural performance monitoring system for the Shanghai Tower", *J. Civil Struct. Health Monit.*, **3**, 49-61.

Yuen, K.V. (2010), *Bayesian methods for structural dynamics and civil engineering*, Wiley, New York.

Yuen, K.V. and Mu, H.Q. (2012), "A novel probabilistic method for robust parametric identification and outlier detection", *Probabilist. Eng. Mech*., **30**, 48-59.

Yuen, K.V. and Katafygiotis, L.S. (2001), "Bayesian time–domain approach for modal updating using ambient data", *Probabilist. Eng. Mech.*, **16**(3), 219-231.

Yuen, K.V. and Katafygiotis, L.S. (2003), "Bayesian fast fourier transform approach for modal updating using ambient data", *Adv. Struct. Eng.*, **6**(2), 81-95.

Yuen, K.V. and Katafygiotis, L.S. (2005), "Model updating using response measurements without knowledge of the input spectrum", *Earthq. Eng. Struct. D.*, **34**(2), 167-187.

Yuen, K.V. and Kuok, S.C. (2010), "Ambient interference in long-term monitoring of buildings", *Eng. Struct.*, **32**, 2379-2386.

Zhang, F.L. and Au, S.K. (2013), "Erratum for fast Bayesian FFT method for ambient modal identification with separated modes by Siu-Kui Au", *J. Eng. Mech. - ASCE*, **139**, 545-545.

Zhang, F.L. and Au, S.K. (2015), "A probabilistic model for modal properties based on operational modal analysis", *ASCE-ASME Journal of Risk and Uncertainty in Engineering Systems, Part A: Civil Engineering*, http://dx.doi.org/10.1061/AJRUA6.0000843. B4015005..

Zhang, F.L. and Au, S.K. (2016), "Fundamental two-stage formulation for Bayesian system identification, Part II: Application to ambient vibration data", *Mech. Syst. Signal Pr.*, **66-67**, 43-61.

BS